ROBUST GPI CONTROLLER FOR TRAJECTORY TRACKING IN A 3RPS PARALLEL ROBOT

ANDRÉS BLANCO-ORTEGA, NORMA C. RUIZ-HIDALGO, JORGE COLIN-OCAMPO, ARTURO ABÚNDEZ-PLIEGO, WILBERTH ALCOCER-ROSADO

Centro Nacional de Investigación y Desarrollo Tecnológico
E-mail: andres.blanco@cenidet.edu.mx, celesterh@cenidet.edu.mx, jcolin@cenidet.edu.mx, abundez@cenidet.edu.mx, wilberth@cenidet.edu.mx

Abstract- Parallel robots have the advantages of handle heavy loads, high rigidity, low inertia and higher accuracy. These robots have been used in applications of motion simulators, machine-tools, fine positioning devices, haptic devices, 3D printers, part handling and spot welding among others. In this paper a configuration of a revolute-prismatic-spherical (RPS) parallel robot with different orientations of the actuators, with respect to other parallel robots reported in the literature, is presented. Robust GPI controller is proposed for trajectory tracking to position the mobile platform in a desired orientation. The simulation results show how the controller is able to compensate non-modeled system disturbances as well as external disturbances.

Index Terms- GPI control, parallel robot, 3 RPS mechanism.

I. INTRODUCTION

Robots have been incorporated into human live little by little, replacing its own tasks. Such as repetitive and dangerous jobs, also in areas that need high precision and time deadline. Also, they are capable of carrying heavy loads and capable of adapting to different tasks. A parallel robot consists of two platforms, one fixed and one mobile, the latter known as end effector or mobile platform. The final effector is linked to the base through independent kinematic chains, which tend to be symmetrical and are attached to the platforms through different types of joints, such as prismatic, revolute, universal and spherical [1].
Parallel robot has many advantages such as stiffness in mechanical structure, stable structure, strong carrying capacity, high position accuracy, fast response, small inertia, low cost, no error accumulation, and can be modular.
Parallel robots are being used in different applications, such as: medical surgeries, rehabilitation systems, motion simulators, human gait simulators, 3D printers, high-precision machining centers, and so forth [2]-[7].
In the literature several works of 3 RPS parallel robots have been reported where the actuators are oriented towards the center in a concurrent manner. Inverse kinematics [8], [9] forward kinematics [10], dynamic model [11] and different control strategies have been reported such as PID control [12], impedance control [13], neuro-fuzzy control [14], adaptive control [15] [16], and computed-torque method [11].

Independent joint controllers (of PD or PID type) are usually employed in industrial robot manipulators but cannot achieve satisfactory performance due to their inherent low rejection to disturbances and parameter variations [17].
Generalized Proportional Integral (GPI) control was introduced, in the context of Predictive Control of Differentially Flat systems in an article by Fliess and his coworkers [18].
GPI controller is proposed for the efficient rejection of a completely unknown perturbation input in a controlled mass system attached to an uncertain mass-spring-damper mechanical system [19].

For other developments concerning GPI control in rehabilitation systems, active vibration control, motor control, inverter are presented in [20]-[24].

The paper is organized in the following order: Section II introduces the model description of the 3RPS parallel robot and the inverse kinematic, in Section III the robust GPI controller for trajectory tracking is proposed. Section IV provides some numerical simulations under MSC Adams environment to show the behavior of the robust controller in a virtual prototype of the parallel robot. Finally, some conclusions are reported in section V.

II. PARALLEL ROBOT DESCRIPTION

A. 3RPS Parallel robot

A 3 degrees of Freedom (DOF) parallel robot structure was design using the RPS configuration [25]. In Fig. 1, shows the virtual prototype of the parallel robot. This robot is formed by 3 electric actuators, 3 revolute joints 3 spherical joints, as well as a mobile platform and a fixed platform.
The configuration of the parallel robot consists in the orientation of the actuators using spherical and revolute joints.

Two actuators are in opposite position, which means that the axes of the revolute joints are parallel; meanwhile the third actuator, is oriented at 90°, or rather, the axis of the revolute joint is 90° turned in relation to the other actuators. The parallel robots proposed by other authors have the actuators oriented to the center of the platform.

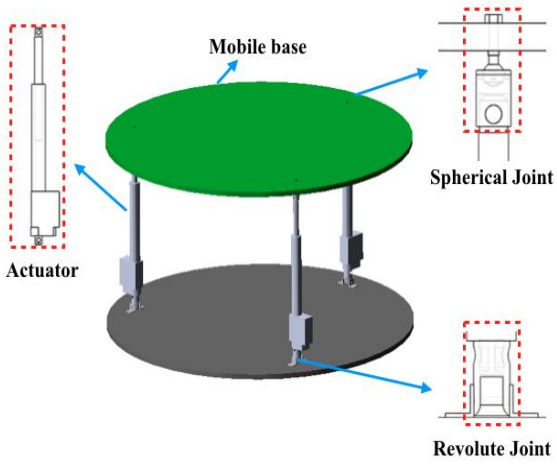


Fig. 1 Configuration of the 3-DOF parallel robot.

B. Inverse kinematic

The inverse kinematics consists in establishing the value of the joint coordinates corresponding to the end-effector configuration (position and orientation). Establishing the inverse kinematics is essential for the position control of parallel robots. The geometric model design of the 3-RPS configuration parallel robot to obtain the inverse kinematic is shown in Fig. 2.

The equations (1) represented the inverse kinematic and were presented in [25].

$$l_1 = k_{e1} + k_4 \sin\beta + k_5 \cos\beta$$

$$l_2 = k_{e1} + k_4 \left(s_{\alpha\theta} \cos\beta - sc_{\beta\theta} \right) + k_5 \left(\cos\alpha - \cos\alpha \cos^2\theta + \cos\beta \cos^2\theta + s_{\alpha\theta} s \right) \quad (1)$$

$$l_3 = k_{e1} - k_4 \left(s_{\alpha\theta} \cos\beta + sc_{\beta\theta} \right) + k_5 \left(\cos\alpha - \cos\alpha \cos^2\theta + \cos\beta \cos^2\theta - s_{\alpha\theta} s \right)$$

where

$$k_1 = h^2,\ k_2 = H^2,\ k_3 = p^2,\ k_4 = -2HP,\ k_5 = -2H \quad (2)$$

$$k_{e1} = k_1 + k_2 + k_3$$

$$s_{\alpha\theta} = \sin\alpha \sin\theta, sc_{\beta\theta} \sin\beta \cos\theta$$

Table 1 shows the parameters of the virtual prototype of the parallel robot and Table II shows the simulation results for inverse kinematic (1) for arbitrary values of α and β.

Table I. Parallel robot parameters

H =0.50 m	p = 0.61 m
h = 0.50 m	$l_1 = l_2 = l_3 = l_0 + \Delta l$
m_1 = 8.9 kg	$l_0 = 0.5$ m
$w = m_1 g$	$\Delta l = 0.23$ m

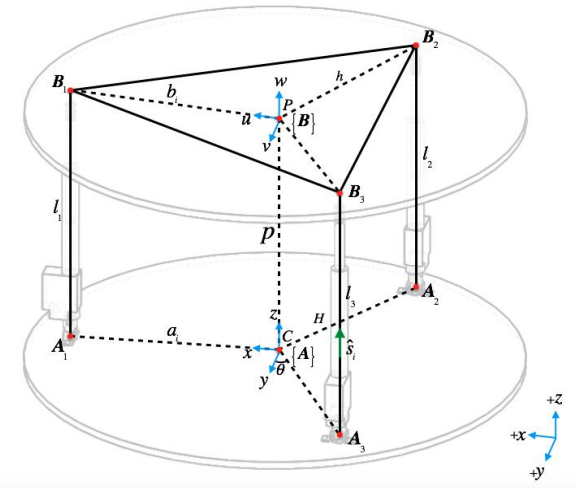


Fig. 2 Geometric model of the 3-RPS parallel robot.

Table II. Results for inverse kinematic

#	l_1 [m]	l_2 [m]	l_3 [m]	α	β
1	0.6131	0.5010	0.7256	15º	0º
2	0.4837	0.6780	0.6780	0º	15º
3	0.5869	0.5362	0.7164	12º	3º
4	0.5434	0.6330	0.6630	2º	8º
5	0.4920	0.6224	0.7254	7º	14º
6	0.5694	0.5599	0.7101	10º	5º
7	0.5434	0.5882	0.7079	8º	8º

III. ROBUST GPI CONTROLLER

C. Dynamic modelling

Obtaining the dynamic model of a parallel robot is complex. On the other hand, some researchers recommend that dynamic models are not used because modeling errors are too numerous [1].

Consider independently each of the actuators that make up the parallel robot, as shown in Fig. 3. The actuator displacement is denoted by z_i (i=1,2,3), b_i is the viscous damping coefficient, F_i is the control input and P_i is considered a disturbance resulting from the mass of the mobile platform and the load may have.

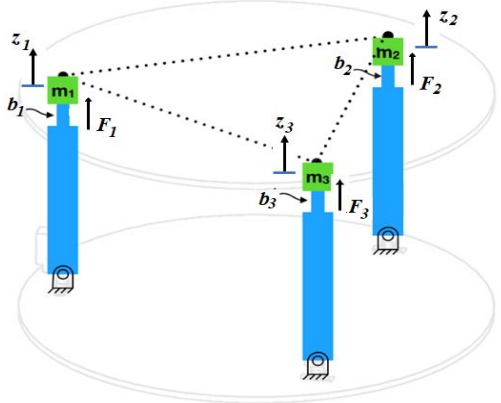


Fig. 3 Schematic diagram of the actuators.

The mathematical models of the actuators can be obtained by applying Newton's second law or Euler-Lagrange formulism and are given by:

$$\begin{aligned} m_1\ddot{z}_1 + b_1\dot{z}_1 &= F_1 + P_1 \\ m_2\ddot{z}_2 + b_2\dot{z}_2 &= F_2 + P_2 \\ m_2\ddot{z}_3 + b_3\dot{z}_3 &= F_3 + P_3 \end{aligned} \quad (1)$$

In order to control the position of the mobile platform of the parallel robot, the actuators are controlled independently. So only the development of the controller design for one actuator will be shown.
Expressing the mathematical model of an actuator as a perturbed system:

$$\ddot{z}_1 = u_1 + \xi_1 \quad (2)$$

Where ξ_1 represents a time polynomial signal of degree 3, of, otherwise, unknown character. The control input is u_1 and z is the output variable.

$$\begin{aligned} u_1 &= \frac{F_1}{m_1} \\ \xi_1 &= \frac{1}{m_1}\left(P_1 - b_1\dot{z}_1\right) \end{aligned} \quad (3)$$

A bounded disturbance is considered due to the mass present in the mobile platform of the form:

$$\xi_1 = a_3t^3 + a_2t^2 + a_1t + a_0 \quad (4)$$

D. Controller design

To compensate the disturbance and achieve the controller's objective of tracking a desired trajectory, the following robust controller is proposed.

$$\begin{aligned} u_1 = {} & \ddot{z}_{1d} - k_5\left(\hat{\dot{z}}_1 - \dot{z}_{1d}\right) - k_4\left(z_1 - z_{1d}\right) - k_3\int_0^t\left(z_1 - z_{1d}\right)d\tau \\ & - k_2\int_0^t\int_0^\tau\left(z_1 - z_{1d}\right)d\lambda d\tau - k_1\int_0^t\int_0^\tau\int_0^\lambda\left(z_1 - z_{1d}\right)d\sigma d\lambda d\tau \\ & - k_0\int_0^t\int_0^\tau\int_0^\lambda\int_0^\sigma\left(z_1 - z_{1d}\right)d\rho d\sigma d\lambda d\tau \end{aligned} \quad (5)$$

where $\hat{\dot{z}}_1$ is an integral reconstructor of the linear velocity of the piston rod, which is given by

$$\begin{aligned} \hat{\dot{z}}_1 &= \int_0^t u_x d\tau \\ \dot{z}_1 &= \hat{\dot{z}}_1 + \dot{z}_{10} \end{aligned} \quad (6)$$

Clearly, a suitable linear combination of up to fourth iterated integrations of the system output tracking error compensates the three-degree time polynomial perturbation input, ξ(t). Substituting the controller (5) and the polynomial representing the disturbance (4) in (2), we get

$$\begin{aligned} \ddot{z}_1 = {} & \ddot{z}_{1d} - k_5\left(\dot{z}_1 - z_{10} - \dot{z}_{1d}\right) - k_4\left(z_1 - z_{1d}\right) \\ & - k_3\int_0^t\left(z_1 - z_{1d}\right)d\tau - k_2\int_0^t\int_0^\tau\left(z_1 - z_{1d}\right)d\lambda d\tau \\ & - k_1\int_0^t\int_0^\tau\int_0^\lambda\left(z_1 - z_{1d}\right)d\sigma d\lambda d\tau \\ & - k_0\int_0^t\int_0^\tau\int_0^\lambda\int_0^\sigma\left(z_1 - z_{1d}\right)d\rho d\sigma d\lambda d\tau \\ & + a_3t^3 + a_2t^2 + a_1t + a_0 \end{aligned} \quad (7)$$

The use of the robust GPI controller (5) yields the following closed-loop dynamics for the trajectory tracking error, $e(t) = z_1 - z_{1d}(t)$:

$$e^{VI} + k_5e^{V} + k_4e^{IV} + k_3\dddot{e} + k_2\ddot{e} + k_1\dot{e} + k_0e = 0 \quad (8)$$

The characteristic equation of the system is now:

$$s^6 + k_5s^5 + k_4s^4 + k_3s^3 + k_2s^2 + k_1s + k_0 = 0 \quad (9)$$

The parameters were selected to ensure that the error dynamics was globally asymptotically stable. We carry out a term by term equalization of the closed loop characteristic polynomial with the desired polynomial, given by:

$$\left(s^2 + 2\varsigma\omega s + \omega^2\right) = 0 \quad (10)$$

with $\varsigma = 1.5, \omega_n = 8$.

E. Trajectory tracking

Desired position trajectory is given by the following Bézier polynomial:

$$\begin{aligned} z_{1d} &= z_i + \left(z_f - z_i\right)\sigma\left(t, t_i, t_f\right)\mu_p^5 \\ \sigma\left(t, t_i, t_f\right) &= \gamma_1 - \gamma_2\mu_p + \gamma_3\mu_p^2 - \cdots + \gamma_6\mu_p^5 \\ \mu_p &= \frac{t - t_i}{t_f - t_i} \end{aligned} \quad (11)$$

where $z_i = z_d\left(t_i\right)$ and $z_f = z_d\left(t_f\right)$ are initial and final desired positions, so that the mobile platform starts from an initial position and go to a final position with a smooth change, such that:

$$z_{1d} = \begin{cases} z_i & 0 \le t < t_i \\ \sigma\left(t, t_i, t_f\right)z_f & t_i \le t < t_f \\ z_f & t > t_f \end{cases} \quad (12)$$

Parameters of the polynomial function (x) are γ1=252, γ2=1050, γ3=1800, γ4=1575, γ 5=700, γ 6=126.

IV. SIMULATION RESULTS

A virtual prototype of the 3 RPS parallel robot [6] was designed and is shown in Fig. 4. Simulations were performed with this virtual prototype under MSC ADAMS software environment to verify the performance of the robust GPI controllers.
The ADAMS program is multibody dynamic analysis software. The 3 RPS parallel robot model is created based on the ADAMS/view.
To set up a co-simulation environment, ADAMS/view provides two modules, ADAMS/Controls and ADAMS/Solver. The ADAMS/Controls module generates a simulation model based on the ADAMS/view model, which can be imported into MALAB/Simulink. During a co-simulation, a closed loop between the ADAMS/view model and control system is formed, as shown in Fig. 5.

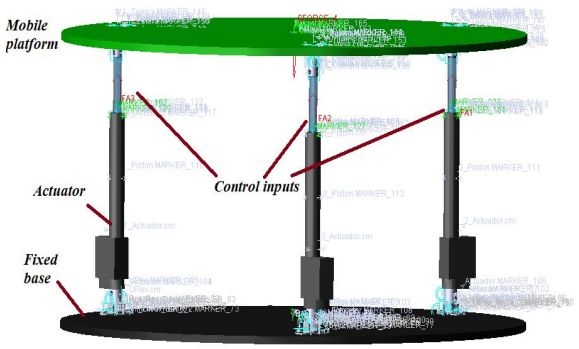


Fig. 4 Virtual prototype under MSC Adams environment.

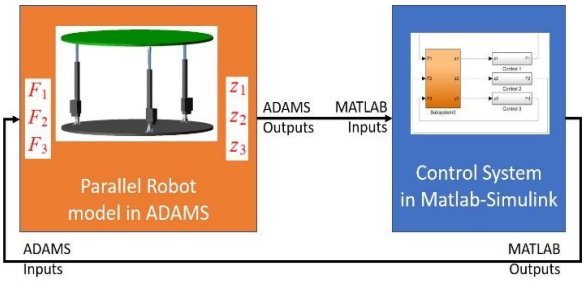


Fig. 5 ADAMS and Matlab in the co-simulation model.

The following figures depicts the response of the virtual prototype of the 3 RPS parallel robot. The simulations are obtained using the robust GPI controller (5) and the Bezier polynomial as desired reference trajectory (12) for the actuator displacements.

F. Simulations results without perturbance

Figure 6 shows the parallel robot response rotating around the x axis, this movement is obtained only by the displacement of the actuator 2 and 3 in the opposite direction (see Figs. 2 and 3). For this movement, from the initial position ($z_1 = z_2 = z_3 = 0.61$ m), the displacements of $z_2 = -0.112$ m and $z_3 = 0.112$ m are required in the actuators (see Fig. 3 and Table II). It can be seen that the displacements of the actuators are smooth to get the orientation of the mobile platform ($\alpha = 15^\circ$).
Note the robust GPI controller for the displacements of the actuators, the tracking error tends to zero, and the movement is smooth. Fig. 7 shows the response for the angular position of the mobile platform for α and β.

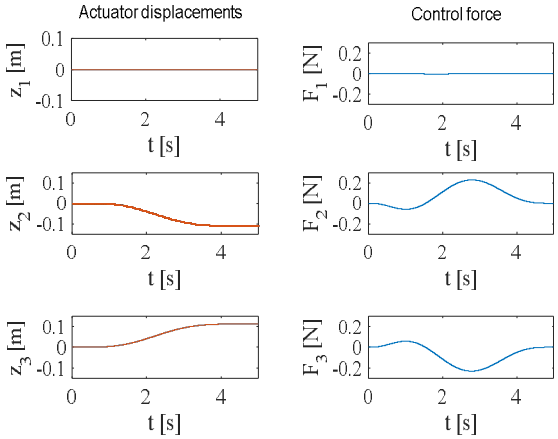


Fig. 6 Displacements and control inputs of the actuators for $\alpha = 15^\circ$.

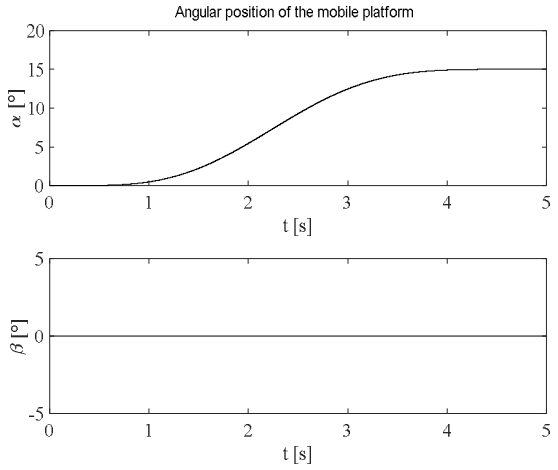


Fig. 7 Response of angular position of the mobile platform for $\alpha = 15^\circ$.

G. Simulations results with perturbance

As a disturbance to the robust GPI controller, the mobile platform mass is modified (55.8 kg) in the virtual prototype. It can be due a load additional in the mobile platform. The controller gains are the same used in the simulation without disturbance.
For simulation results shows in Fig. 8, the trajectories for the desired displacements are the same as those used in Fig. 6. Note the robust GPI controller for the displacements of the actuators, the tracking error tends to zero, and the movement is smooth. The robust

controller rejects the disturbance increasing three times with respect to the response of the parallel robot without disturbance. The displacements of the actuators and the control inputs to position the mobile platform ($\alpha = 15^\circ$) is shown in Fig. 8. The angular positioning of the mobile platform is shown in Fig. 9.

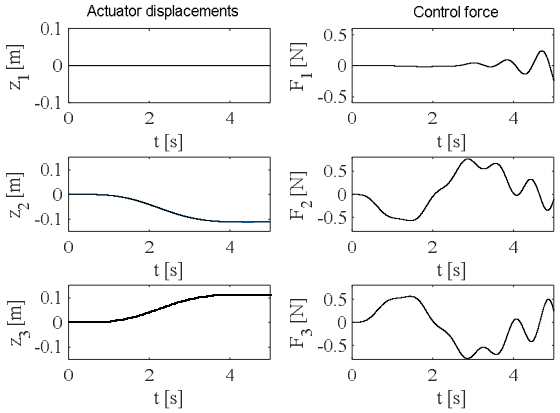


Fig. 8 Displacements and control inputs of the actuators for $\alpha = 15^\circ$ with disturbance in the mobile platform mass.

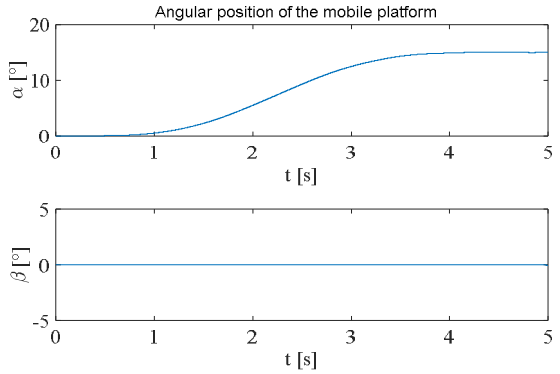


Fig. 9 Response of angular position of the mobile platform for $\alpha = 15^\circ$ with disturbance in the mobile platform mass.

Fig. 10 and Fig. 11 show the response for the mobile platform of the parallel robot to achieve the desired angles ($\alpha = \beta = 15^\circ$). In this case, the actuator 1 must be negative and the actuators 2 and 3 must have a positive value, see Fig. 3 and Table II. In these simulation results there is an error in tracking the desired trajectory.

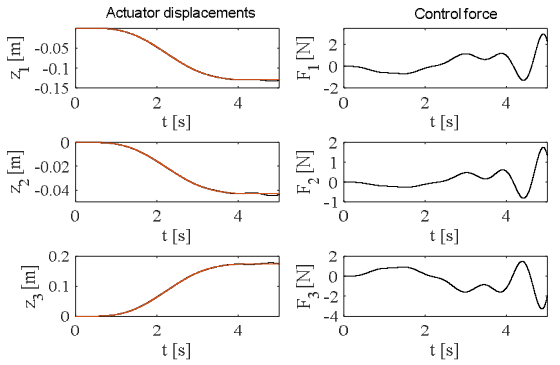


Fig. 10 Displacements and control inputs of the actuators for $\alpha = 15^\circ$ and $\beta = 15^\circ$.

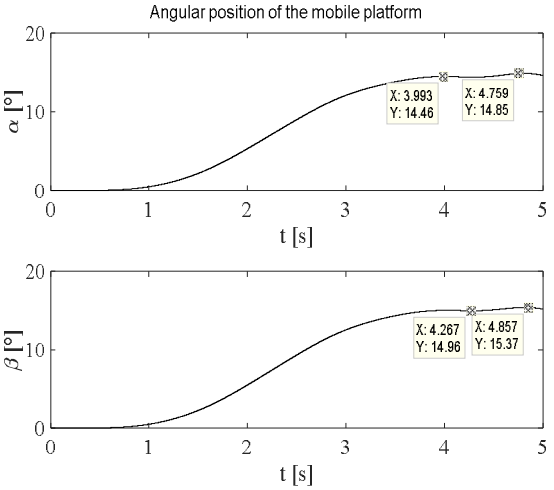


Fig. 11 Response of angular position of the mobile platform for $\alpha = 15^\circ$ and $\beta = 15^\circ$.

CONCLUSION

In this paper, a control strategy for a 3 RPS parallel robot based on generalized proportional integral (GPI) controllers is presented, and the performance of the control system has been evaluated by means of simulations.

The simulation results are obtained from the virtual prototype simulated under the ADAMS environment using the robust GPI controller. An increase in the mass of the mobile platform is considered as disturbance for the controller. The control strategy demonstrated that it is able to guarantee the trajectory tracking task during the positioning of the mobile platform of the parallel robot. These simulations show the effectiveness of the proposed controller.

ACKNOWLEDGMENT

Research reported here was supported by grants of the Tecnológico Nacional de México, TecNM through Fortalecimiento de Cuerpos Académicos 2017 with the project " Diseño y construcción de un robot paralelo para el anaveaje", IDCA 24320, CENIDET-CA-16

REFERENCES

[1] J. P. Merlet, “Parallel Robots,” Second Edition. Springer Netherlands, 2006.

[2] Jamwal PK, Hussain S, Ghayesh MH, Rogozina SV. “Adaptive Impedance Control of Parallel Ankle Rehabilitation Robot”. ASME. J. of Dynamic Systems, Measurement, and Control; 139(11):111006-111006-7, 2017.

[3] B. Guo, H. Jin, P. Zhang, J. Zhang, Y. Hu and H. Zhang, "Accuracy analysis and calibration of a parallel guidance device for minimal invasive spinal surgery," 2013 IEEE International Conference on Robotics and Biomimetics (ROBIO), pp. 1468-1473, Shenzhen, 2013.

[4] B. Li, H. Jin, M. Fang, Y. Hu and P. Zhang, "Spinal physiological motion simulator and compensation method for a robotic spinal surgical system," 2014 IEEE International Conference on Robotics and Biomimetics (ROBIO 2014), pp. 229-234, Bali, 2014.

[5] Cao, R., Gao, F., Zhang, Y., Pan, D., Chen, W. “A new parameter design method of a 6-DOF Parallel Motion Simulator for a Given Workspace”. Mechanics Based Design of Structures and Machines 43(1):1-18, 2015.

[6] Dan Zhang, S. Patel, Zhen Gao and Yunjian Ge, "Stiffness control for a 3-DOF parallel robot based machine tools," 2008 International Conference on Information and Automation, pp. 1085-1090, Changsha, 2008.

[7] R. Celi, A. Sempértegui, D. Morocho, D. Loza, D. Alulema and M. Proaño, "Study, design and construction of a 3D printer implemented through a delta robot," 2015 CHILEAN Conference on Electrical, Electronics Engineering, Information and Communication Technologies (CHILECON), pp. 717-722, Santiago, 2015.

[8] X. Li, D. Zhu, Z. Mei and D. Jiang, "Kinematic analysis of 3-RPS parallel mechanism," 2017 2nd International Conference on Robotics and Automation Engineering (ICRAE), pp. 183-187, Shanghai, 2017.

[9] L. Yu, L. Zhang, N. Zhang, S. Yang and D. Wang, "Kinematics simulation and analysis of 3-RPS parallel robot on SimMechanics," The 2010 IEEE International Conference on Information and Automation, pp. 2363-2367, Harbin, 2010.

[10] S. H. Mirmohammad, A. Yousefi-Koma and S. S. Mohtasebi, "Direct kinematics of a three revolute-prismatic-spherical parallel robot using a fast homotopy continuation method," 2016 4th International Conference on Robotics and Mechatronics (ICROM), pp. 410-415, Tehran, 2016.

[11] M. Shahidi, J. Keighobadi, A. R. Khoogar, “3-RPS Parallel Manipulator Dynamical Modelling and Control Based on SMC and FL Methods,” AUT J. Modeling and Simulation, 49(2), 217-226, 2017.

[12] D. Verde, S. D. Stan, M. Manic, R. Balan and V. Matie, "Kinematics analysis, workspace, design and control of 3-RPS and TRIGLIDE medical parallel robots," 2009 2nd Conference on Human System Interactions, Catania, 2009, pp. 103-108.

[13] H. Z. Arabshahi and A. B. Novinzadeh, "Impedance control of the 3RPS parallel manipulator," 2014 Second RSI/ISM International Conference on Robotics and Mechatronics (ICRoM), pp. 486-492, Tehran, 2014.

[14] Y. Fan and Y. Yin, "Mechanism design and motion control of a parallel ankle joint for rehabilitation robotic exoskeleton," 2009 IEEE International Conference on Robotics and Biomimetics (ROBIO), pp. 2527-2532, Guilin, 2009.

[15] Guoliang Tao, Ce Shang, and Deyuan Meng, “Adaptive Robust Posture Control of a 3-RPS Pneumatic Parallel Platform with Unknown Deadzone,” Mathematical Problems in Engineering, vol. 2016, Article ID 2034923, 16 pages, 2016.

[16] Ce Shang, Guoliang Tao and Deyuan Meng, “Adaptive robust trajectory tracking control of a parallel manipulator driven by pneumatic cylinders,” Advances in Mechanical Engineering, Vol. 8(4) 1–15, 2016.

[17] P. Chiacchio, F. Pierrot, L. Sciavicco and B. Siciliano, "Robust design of independent joint controllers with experimentation on a high-speed parallel robot," in IEEE Transactions on Industrial Electronics, vol. 40, no. 4, pp. 393-403, Aug 1993.

[18] M. Fliess, R. Marquez, E. Delaleau and H. SiraRamírez, “Correcteurs Proportionnels–Integraux Généralisés," ESAIM Control, Optimisation and Calculus of Variations, Vol. 7, No. 2, pp. 23-41, 2002.

[19] H. Sira-Ramírez, F. Beltrán-Carbajal, and A. Blanco-Ortega, “Robust generalized proportional integral controller for the induction motor,” in Proc. of the 10th International Workshop on Variable Structure Systems, Antalya, Turkey, June 2008.

[20] F. Beltrán-Carbajal, E. Chávez-Conde, A. F. Contreras, R. F. Vázquez-Bautista. “Active perturbation rejection in motion control of milling machine tools,” Rev. Fac. Ing. Univ. Antioquia, 69 (1) pp. 193-204, 2013.

[21] C. H. Guzmán, A. Blanco, J. A Brizuela, F. A. Gómez “Robust control of a hip-joint rehabilitation robot”. Biomedical Signal Processing & Control 35: 100-109, 2017.

[22] A. Blanco Ortega, L. G. Vela Valdés, G. López López and A. Magadán Salazar, "A Generalized Proportional Integral Controller for the Robust Perturbation Rejection in an Ankle Rehabilitation Machine," 2013 International Conference on Mechatronics, Electronics and Automotive Engineering, pp. 140-145, Morelos, 2013.

[23] H. Sira-Ramirez, F. Beltran-Carbajal and A. Blanco-Ortega, "A robust generalized proportional integral controller for the induction motor," 2008 International Workshop on Variable Structure Systems, pp. 89-94, Antalya, 2008.

[24] J. A. Juárez-Abad, J. Linares-Flores, E. Guzmán-Ramírez and H. Sira-Ramírez, "Generalized Proportional Integral Tracking Controller for a Single-Phase Multilevel Cascade Inverter: An FPGA Implementation," in IEEE Transactions on Industrial Informatics, vol. 10, no. 1, pp. 256-266, Feb. 2014.

[25] N. C. Ruiz-Hidalgo, A. Blanco-Ortega, A. Abúndez-Pliego, J. Colin-Ocampo, and M. Arias-Montiel, “Design and Control of a Novel 3-DOF Parallel Robot,” in 2016 International Conference on Mechatronics, Electronics and Automotive Engineering Design, pp. 66–71, 2016.

★★★